# The Metalation of (*tert*-Butyldimethylsilyl)(2-pyridylmethyl)amine with Dimethylzinc and Subsequent Zinc-Mediated Carbon−Carbon Coupling Reaction

**Matthias Westerhausen,*[a] Tobias Bollwein,[a] Nikolaos Makropoulos,[a] Thomas M. Rotter,[a] Tassilo Habereder,[a] Max Suter,[a] and Heinrich Nöth[a]**

**Keywords:** Amides / Zinc / C−C coupling / Metalations / Metallacycles / N ligands

The lithiation of 2-(aminomethyl)pyridine and the subsequent reaction with $ClSiMe_2tBu$ yields (*tert*-butyldimethylsilyl)(2-pyridylmethyl)amine (**1**). The metalation of **1** with dimethylzinc gives colorless dimeric methylzinc 2-pyridylmethyl(*tert*-butyldimethylsilyl)amide (**2**), which crystallizes in the triclinic space group $P\bar{1}$. The solvent-free thermal decomposition of **2** at 150 °C leads to the evolution of methane, the precipitation of zinc metal and the formation of amine **1**, bis(methylzinc)—1,2-dipyridyl-1,2-bis(*tert*-butyldimethylsilylamido)ethane (**3**), and bis[(*tert*-butyldimethylsilyl)(2-pyridylmethyl)amido]zinc (**4**). Compound **3** can be obtained in good yield by reacting **2** with dimethylzinc at elevated temperatures in toluene. During this reaction, zinc metal precipitates and methane is evolved. The C–C coupling product **3** crystallizes in the tetragonal space group $I4_1cd$. The lithiation of **1** and the subsequent metathesis reaction with anhydrous $ZnCl_2$ yields complex **4** almost quantitatively.

## Introduction

Pyridine complexes of zinc compounds are a well-known class of substance. On the one hand pyridine, as well as its derivatives such as 2,2′-bipyridine, are able to stabilize dialkylzinc[1−3] or even a geminal biszincated alkane but,[4] on the other hand, these coligands support homolytic Zn−C bond cleavage upon irradiation.[5] Furthermore, multi-dentate azaligands such as, for example, trispyrazolylborate anions enable reactions at the metal centers that can serve as model systems for enzymes.[6]

The reaction of dialkylzinc with 1,4-di(*tert*-butyl)-1,4-diazabutadiene (DAB) or *N*-*tert*-butylpyridine-2-carbaldimine (PYCA) yields the corresponding 1:1 complexes, which are red in color.[7] Subsequent to the adduct formation these compounds have three possible reaction pathways depending on the zinc-bonded alkyl substituent and on the reaction conditions: *C*-alkylation (**A**), *N*-alkylation (**B**) and homolytic Zn−C bond cleavage (**C**) (Scheme 1).[7,8,9] During all these reactions, one alkylzinc moiety remains unchanged and can be regarded as a spectator because the coordination of this metal fragment to the nitrogen atoms of the chelating ligand remains unchanged. Precipitation of zinc metal was not reported to occur during the course of the reactions.

Complex **C** shows a monomer-dimer equilibrium. The dimerization occurs through C−C bond formation as shown in Scheme 2. The newly formed C−C bond is longer than a C−C single bond, as exemplified by [Et−Zn(PYCA)]$_2$ with 156.9(8) pm and [$Me_3SiCH_2$−Zn(DAB)]$_2$ with a longer distance of 162 pm.[10]

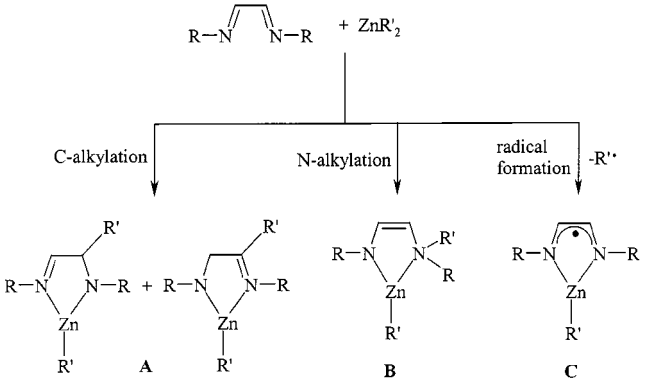


Scheme 1. Possible reaction pathways of dialkylzinc with 1,4-di(*tert*-butyl)-1,4-diazabutadiene.

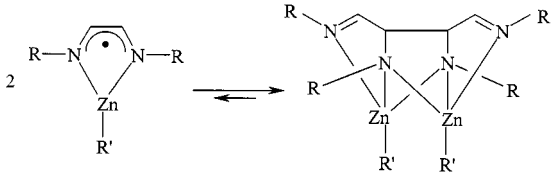


Scheme 2. Monomer-dimer equilibrium through C−C bond cleavage and formation.

The reduction of 1,4-di(*tert*-butyl)-1,4-diazabutadiene with lithium and the subsequent metathesis reaction with (DAB)$ZnCl_2$ yields $Zn(DAB)_2$, which can easily be reduced with potassium or oxidized in a comproportionation with (DAB)$Zn(O_3S-CF_3)_2$.[11] During all these reaction sequences, which were reported by van Koten and co-workers, the oxidation state of +2 for zinc remains unchanged.

Here we report on the synthesis of (*tert*-butyldimethylsilyl)(2-pyridylmethyl)amine, which can easily be metalated

[a] Department Chemie der Ludwig-Maximilians-Universität, Munich,
Butenandtstraße 9 (House D), 81377 Munich, Germany
Fax: (internat.) + 49-(0)89/2180−7867
E-mail: maw@cup.uni-muenchen.de

  1434−1948/01/0303−0851 $ 17.50+.50/0 

by dimethylzinc. The thermal decomposition as well as the reaction of this product with excess dimethylzinc leads to C−C bond formation and the precipitation of an equimolar amount of zinc metal. This unusual oxidative carbon−carbon coupling under formation of $Zn^0$ is irreversible and evidence for a monomer−dimer equilibrium by homolytic C−C bond cleavage was not found. The zincation of 2-(*N*-*tert*-butylaminomethyl)-1-methylbenzimidazole also uses the chelate effect and a zinc atom with a coordination number of 3 can be stabilized.[12] However, C−C bond formation was not observed during this reaction.

## Results and Discussion

### Synthesis

The lithiation of 2-pyridylmethylamine and the subsequent metathesis reaction with *tert*-butyldimethylsilyl chloride quantitatively yields (*tert*-butyldimethylsilyl)(2-pyridylmethyl)amine (**1**). Zincation of **1** with dimethylzinc in toluene gives colorless dimeric methylzinc—(*tert*-butyldimethylsilyl)(2-pyridylmethyl)amide (**2**) according to Scheme 3.

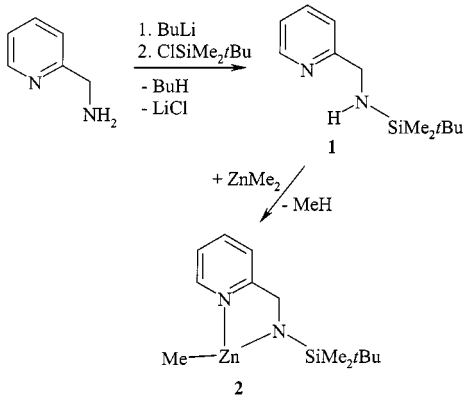


Scheme 3. Synthesis of **1** and **2**

The thermal decomposition of molten **2** at approximately 150 °C (Scheme 4) leads to the evolution of methane, as confirmed by mass spectrometry. During the course of this reaction the precipitation of zinc metal is observed and the NMR spectroscopic data also indicate the formation of **1**. In addition to these substances two new compounds are formed, namely the C−C coupling product bis(methylzinc)—1,2-bis(*tert*-butyldimethylsilylamido)-1,2-dipyridylethane (**3**) and bis[(*tert*-butyldimethylsilyl)(2-pyridylmethyl)-amido]zinc (**4**). Complex **4** forms due to zincation of (*tert*-butyldimethylsilyl)(2-pyridylmethyl)amine (**1**) by derivative **2** under elimination of methane, as shown in Scheme 5. The C−C coupling product and the elemental zinc are formed in an equimolar ratio. Scheme 4 represents the reaction sequence of this thermolysis of **2** and the $^1H$ NMR spectrum of the thermolysis reaction is presented in Figure 1. The subsequent addition of dimethylzinc leads to the metalation of **1** and to dismutation reactions with **4**, both of which lead to **2**. The isolation of analytically pure **4** by fractional crystallization was not possible due to co-precipitation of minor amounts of **2** and/or **3** in the sample. For the sake of comparison, compound **4** was prepared by the metathesis reaction of anhydrous $ZnBr_2$ with lithium 2-pyridylmethyl-(*tert*-butyldimethylsilyl)amide, which was generated in situ by lithiation of **1**.

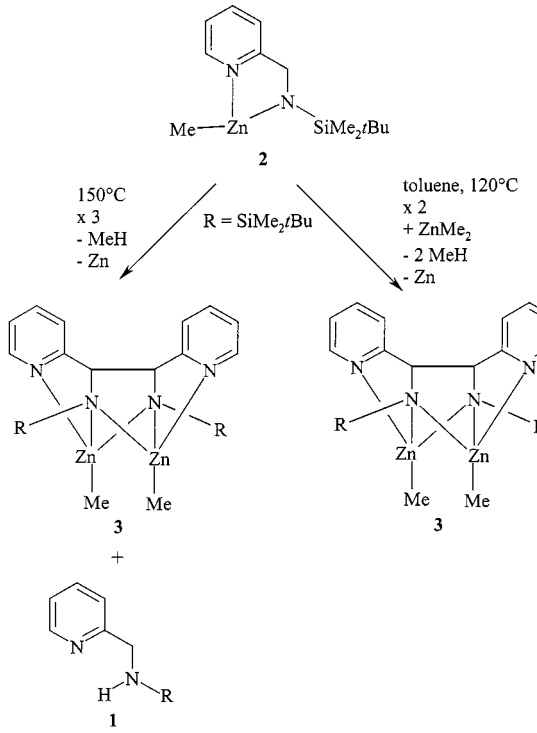


Scheme 4. Synthesis of the C−C coupling product **3** by reaction of **2** with dimethylzinc and as a result of thermal decomposition of **2** at 150 °C, which also gives complex **4** due to the metalation of **1** with **2** in the melt.

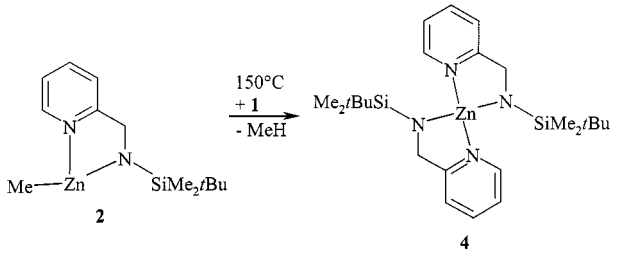


Scheme 5

In order to avoid the formation of bis[2-pyridylmethyl-(*tert*-butyldimethylsilyl)amido]zinc (**4**) and to obtain quantitatively the C−C coupling product **3**, dimethylzinc is added prior to the thermolysis of **2** in refluxing toluene. In this case neither amine **1** nor complex **4** are detectable by NMR spectroscopy, as shown in Figure 1. The zincation of the $CH_2$ group and the oxidative C−C coupling reaction lead to the precipitation of zinc metal, as confirmed by X-ray powder diffraction methods (Figure 2). The use of a molar ratio of 3:2 for dimethylzinc and (*tert*-butyldimethylsilyl)(2-pyridylmethyl)amine (**1**) gives **3** and elemental zinc in a 1:1 molar ratio.

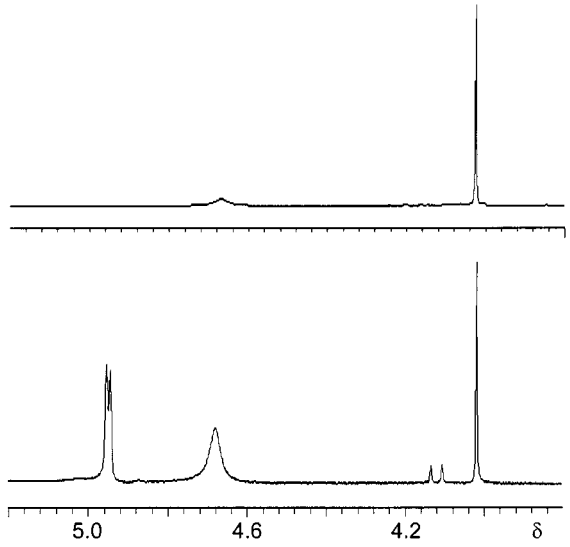


Figure 1. $^1$H NMR spectroscopic monitoring of the progress of the C−C coupling reaction shown in the region of δ = 4.0 to 5.1 at 30 °C. Upper spectrum: Reaction of **2** with dimethylzinc in toluene; only compounds **2** and **3** are observed. Lower spectrum: Spectrum after thermal decomposition of **2** at 150 °C for 2 hours; after dissolving the residue in toluene compounds **1**, **3**, and **4** are detected (see also Table 2).

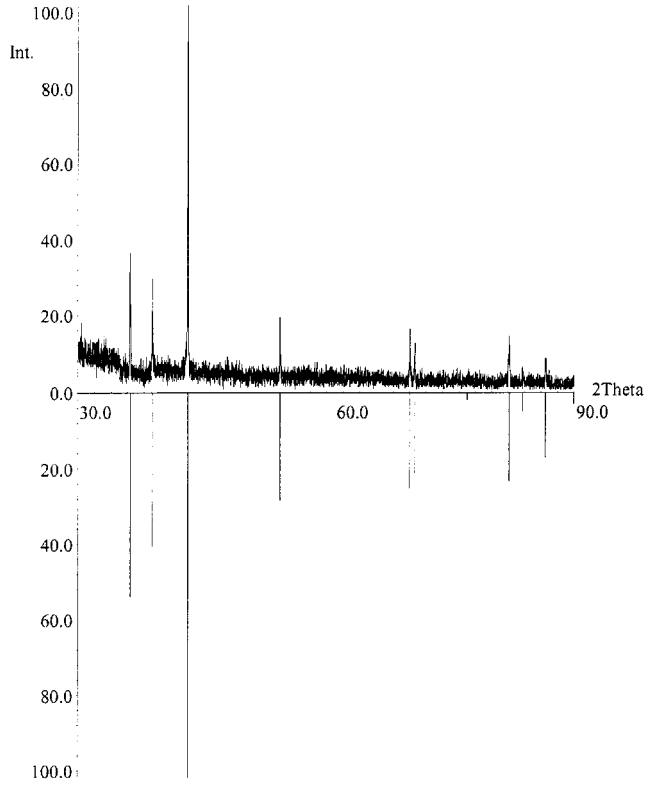


Figure 2. X-ray powder diffractogram of zinc that precipitated during the C−C coupling reactions (upper spectrum) and the reference line spectrum (below).

The stereoselective C−C coupling reaction leads to the formation of the *R*,*R* and *S*,*S* enantiomers, whereas a *meso*-diastereomer was not observed. A similar product with *tert*-butyl substituents at the nitrogen atoms was obtained by metalation of the corresponding amine and was already reported by van Koten and co-workers.[10] However, this complex dissociates into monomeric radicals through a homolytic C−C bond cleavage, as shown in Scheme 2. The presence of trialkylsilyl substituents seems to prevent this monomerization process. The colorless C−C coupling product **3** is EPR silent and its solution is colorless. In order to investigate the influence of the C−C coupling reaction on the coordination spheres of zinc and the amide nitrogen atoms the crystal structure determinations of **2** and **3** were performed.

### Molecular Structures of 2 and 3

The molecular structure of **2** is shown in Figure 3 along with the numbering scheme. The second half of the molecule is generated by inversion symmetry and these atoms are marked with apostrophes. The zinc atom Zn1 is coordinated tetrahedrally by three nitrogen atoms and a methyl group. Selected bond lengths and angles are given in Table 1.

Due to the inversion symmetry the central $Zn_2N_2$ cycle is planar with an N1−Zn1−N1′ angle of 94°. The Zn−C distances lie within a characteristic range and there is no sign of steric strain in this dimer, although the Zn−N bonds are slightly longer than those in the aminomethylpyridine complexes of the zinc dihalides[13] and much longer than those in homoleptic zinc bis(amides).[14]

Figure 4 shows the molecular structure and the numbering scheme of the C−C coupling product **3**. The second half of the molecule is generated by crystallographic $C_2$ symmetry and the generated atoms are marked with apostrophes. Selected structural data are presented in Table 2. For the sake of comparison the numbering schemes of **2** and **3** are alike.

A tetradentate aza ligand is formed in the C−C coupling. Therefore, the methyl groups at the zinc atoms are at the same side of the $Zn_2N_2$ cycle. The C7 atom is chiral. Due to the molecular $C_2$ symmetry and the noncentrosymmetric

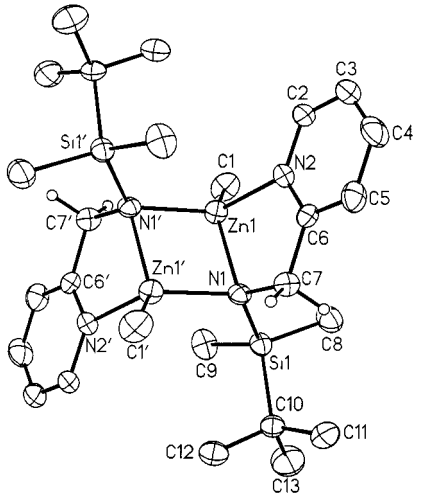


Figure 3. Molecular structure of **2**. The ellipsoids represent a probability of 40%. Atoms generated by the crystallographic inversion symmetry (−*x*, −*y*, −*z* + 1) are marked with apostrophes. The hydrogen atoms are omitted for clarity (with the exception of those at C7/C7′).

Table 1. Selected bond lengths [pm] and angles [°] of **2** and **3**

| | 2 | 3 |
|---|---|---|
| Zn1−C1 | 199.1(9) | 196.4(3) |
| Zn1−N2 | 208.2(7) | 211.1(2) |
| Zn1−N1 | 211.7(6) | 215.7(2) |
| Zn1−N1′ | 209.7(6) | 208.8(2) |
| N1−Si1 | 174.0(6) | 172.4(2) |
| N1−C7 | 145(1) | 145.7(3) |
| N2−C2 | 136.3(9) | 134.3(3) |
| N2−C6 | 135(1) | 134.9(3) |
| C2−C3 | 137(1) | 136.7(4) |
| C3−C4 | 137(2) | 136.5(4) |
| C4−C5 | 139(1) | 139.2(3) |
| C5−C6 | 139(1) | 137.8(3) |
| C6−C7 | 152(1) | 153.8(3) |
| C7−C7′ | - | 156.7(4) |
| C1−Zn1−N1 | 131.9(3) | 135.5(1) |
| C1−Zn1−N1′ | 119.1(3) | 131.1(1) |
| C1−Zn1−N2 | 112.4(4) | 121.1(1) |
| N1−Zn1−N1′ | 94.0(2) | 75.10(8) |
| N1−Zn1−N2 | 82.4(2) | 81.55(7) |
| N1′−Zn1−N2 | 111.1(2) | 96.56(8) |
| Si1−N1−Zn1 | 110.8(3) | 120.9(1) |
| Si1−N1−Zn1′ | 124.8(3) | 122.8(1) |
| Si1−N1−C7 | 113.6(5) | 120.3(2) |
| Zn1−N1−Zn1′ | 86.0(2) | 79.73(7) |
| Zn1−N1−C7 | 110.0(4) | 94.9(1) |
| Zn1′−N1−C7 | 107.9(5) | 108.3(1) |

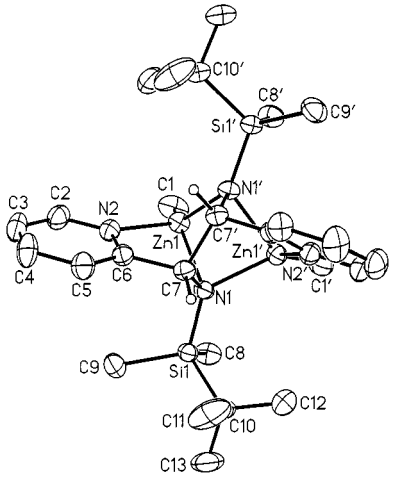


Figure 4. Molecular structure and numbering scheme of **3**. The ellipsoids represent a probability of 40%. Atoms generated by the crystallographic $C_2$ symmetry ($-x + 1 - 1$, $-y + 1$, $z + 1 - 1$) are marked with apostrophes. The hydrogen atoms are omitted for clarity (with the exception of those at C7/C7′).

tetragonal space group $I4_1cd$, the crystalline compound of this material consists of the *R*,*R* enantiomer. The arrangement of the molecules in the solid state is shown in Figure 5 and it can be seen that the molecules are orientated in the same direction.

The newly formed C7−C7′ bond of **3** is rather long, a situation also observed for $[Et-Zn(PYCA)]_2$ and $[Me_3SiCH_2-Zn(DAB)]_2$.[10] The tetradentate aza ligand enforces strong deviations from planarity in the $Zn_2N_2$ cycle. The angle between the normals of the planes N1/Zn1/N1′ and N1/Zn1′/N1′ amounts to 72.1°. This leads to short transannular Zn1Zn1′ contacts [287.5(2) pm for **2** and 272.11(5) pm for **3**] and small endocyclic angles at Zn1 and N1 (Table 1). The environment of C7 shows only insignificant deviations from the tetrahedral geometry.

Table 2. Selected NMR spectroscopic data of (*tert*-butyldimethylsilyl)(2-pyridylmethyl)amine (**1**), the metalation product **2**, the C−C coupling product **3**, and bis[2-pyridylmethyl(*tert*-butyldimethylsilyl)amido]zinc (**4**).

| Compound | 1 | 2 | 3 | 4 |
|---|---|---|---|---|
| $^1$H : | | | | |
| δ(H1) | – | −0.25 | −0.51 | – |
| δ(H2) | 8.47 | 8.25 | 7.98 | 7.95 |
| δ(H3) | 6.68 | 6.47 | 6.48 | 6.38 |
| δ(H4) | 7.17 | 6.85 | 6.97 | 6.84 |
| δ(H5) | 7.06 | 6.52 | 6.77 | 6.64 |
| δ(H7) | 4.09 | 4.65 | 4.03 | 4.93[a] |
| δ(H8) | 0.01 | −0.11 | 0.40 | 0.34 |
| δ(H9) | 0.01 | −0.11 | 0.15 | 0.28 |
| δ($CMe_3$) | 0.87 | 1.10 | 0.82 | 1.27 |
| $^{13}$C{$^1$H} | | | | |
| δ(C1) | – | −12.64 | −14.07 | – |
| δ(C2) | 148.88 | 145.44 | 146.66 | 145.64 |
| δ(C3) | 121.03 | 121.67 | 122.38 | 122.03 |
| δ(C4) | 135.71 | 137.54 | 138.36 | 136.16 |
| δ(C5) | 120.45 | 121.49 | 119.89 | 121.10 |
| δ(C6) | 163.24 | 165.49 | 168.49 | 166.44 |
| δ(C7) | 48.21 | 54.09 | 67.27 | 54.39 |
| δ(C8) | −5.04 | −3.57 | −2.06 | −3.03 |
| δ(C9) | −5.04 | −3.57 | −3.23 | −3.30 |
| δ(C10) | 18.47 | 20.83 | 20.59 | 20.84 |
| δ($CMe_3$) | 26.25 | 28.59 | 27.68 | 28.08 |
| $^{29}$Si{$^1$H} | | | | |
| δ(Si) | 9.04 | 10.32 | 8.66 | 3.92 |

[a] Mean value of an AB spin system, δ = 4.91; δ = 4.95; $^2J(H_A,H_B)$ = 19.9 Hz.

## NMR Spectroscopy

The NMR parameters of these compounds are listed in Table 2. The numbering scheme is taken from the X-ray structures presented in Figure 3 and 4 for **2** and **3**, respectively. The hydrogen atoms carry the same numbers as the corresponding carbon atoms. A similar numbering scheme is applied to **1** and **4**.

The C−C coupling and the resulting higher steric strain on the zinc centers lead to a high-field shift of the signals due to the zinc-bonded methyl groups in both the $^1$H and the $^{13}$C{$^1$H} NMR spectra. The signals due to the silicon-bonded methyl substituents of **2** are shifted to higher field compared to **1**, whereas the methyl groups of **3** are more deshielded. Furthermore, two singlets are observed for the methyl groups at the Si atoms for **3** and **4**. Compounds **2** and **4**, which both contain the bidentate (*tert*-butyldimethylsilyl)(2-pyridylmethyl)amide substituent, are easily identified by their δ($^{29}$Si{$^1$H}) values.

The most sensitive NMR probe for these molecules is the C7/H7 moiety and therefore this region was chosen to monitor the thermal decomposition of **2** (Figure 1). The AB spin system for the methylene group in **4** results from the tetrahedral geometry at the zinc atom: One hydrogen atom at C7 is at the same side as the pyridyl group of the opposite ligand, whereas the other H atom is oriented to the side of the trialkylsilyl group. The geminal coupling constant has a

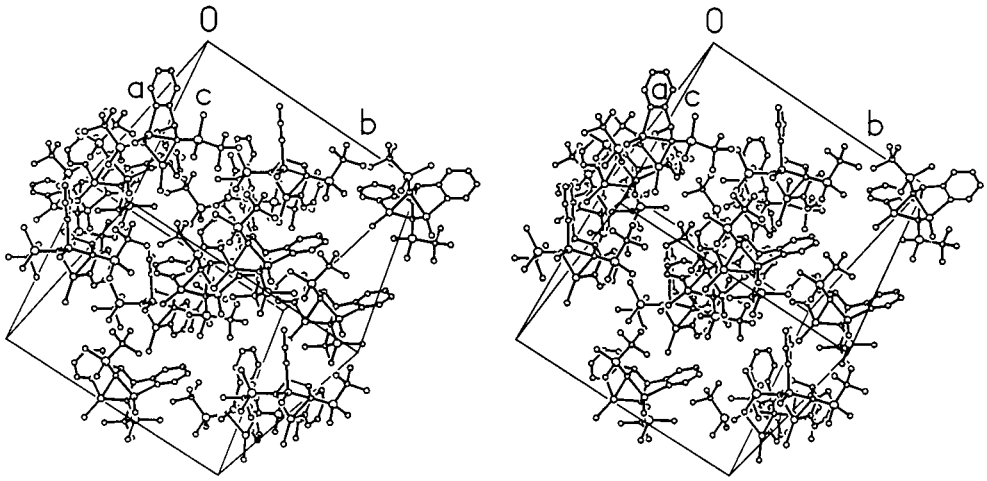


Figure 5. Stereoscopic view of the arrangement of the molecules of **3** in the elementary cell. All atoms are drawn with arbitrary radii, the H-atoms are omitted for clarity.

value of approximately 20 Hz and lies in the expected range. The $^{13}C$ chemical shifts of C7 vary between $\delta = 48.2$ for (*tert*-butyldimethylsilyl)(2-pyridylmethyl)amine (**1**) and $\delta = 67.3$ for the C−C coupling product **3**.

## Conclusion and Prospects

The zincation of (*tert*-butyldimethylsilyl)(2-pyridylmethyl)-amine (**1**) quantitatively yields **2**. The thermolysis of this compound, as well as the reaction of **2** with dimethylzinc, leads to oxidative C−C bond formation and yields **3**. At the same time the precipitation of an equimolar amount of zinc metal is observed. The synthetic approach to compound **3** is different to the synthesis of (PYCA)ZnEt reported by van Koten and co-workers. In contrast to bis(alkylzinc)—1,2-bis(*tert*-butylamido)-1,2-dipyridylethane, a monomer-dimer equilibrium is not observed for **3**. This allows the investigation of the reactivity of two zinc atoms that are in close contact with each other without considering the chemistry of radicals, which would form due to the homolytic C−C bond cleavage.

## Experimental Section

**General Remarks:** All experiments and manipulations were carried out under an argon atmosphere. Reactions were performed using standard Schlenk techniques and the solvents were dried and thoroughly deoxygenated prior to use. − NMR spectra were recorded on Jeol GSX270 and EX400 spectrometers. − A Nicolet 520 FT-IR spectrophotometer was used to record the IR spectra; solid substances were analysed in nujol between KBr plates (vs very strong, s strong, m medium strong, w weak, vw very weak, sh shoulder). − The low carbon and nitrogen values in the elemental analyses result from the presence of carbide and carbonate as well as nitride formation during combustion of the compounds.

**(*tert*-Butyldimethylsilyl)(2-pyridylmethyl)amine (1):** A 2.5 M solution of *n*-butyllithium in hexane (40 mL, 100 mmol) was added slowly to a precooled solution (−78 °C) of 10.8 g of 2-aminomethylpyridine (100 mmol) in 100 mL of tetrahydrofuran. After 5 minutes of stirring, a solution of 15.1 g of *tert*-butyldimethylsilyl chloride (100 mmol) in 25 mL of tetrahydrofuran was added at −78 °C. The reaction solution was allowed to warm up and stirred at room temperature for an additional 2 h. The solvent was removed in vacuo at room temperature. The residue was dissolved in pentane and any insoluble materials were filtered off. The volatile components were removed at 120 °C to leave **1** as an oil which is an only slightly air-sensitive oil; yield: 19.54 g (87.9 mmol), 88%. − NMR spectroscopic data are listed in Table 2. − IR: $\tilde{\nu} = 3370$ cm$^{-1}$ br, 3084 sh, 3069 w, 3010 w, 2953 s, 2928 s, 2896 s, 2883 s, 2855 s, 1593 s, 1571 m, 1471 s, 1463 s, 1434 s, 1406 s, 1388 s, 1360 m, 1344 w, 1254 s, 1216 w, 1145 sh, 1125 s, 1093 m, 1085 m, 1047 m, 1006 m, 995 m, 955 w, 938 m, 884 sh, 832 s, 812 m, 776 s, 752 m, 726 w, 680 w, 662 m, 628 w, 595 w, 565 w, 456 w, 403 w, 374 br, 358 br. − $C_{12}H_{22}N_2Si$ (222.406): calcd. C 64.80, H 9.97, N 12.59; found C 63.88, H 9.62, N 12.56.

**Methylzinc—2-Pyridylmethyl(*tert*-butyldimethylsilyl)amide (2):** A 2.0 M solution of dimethylzinc in toluene (4.8 mL, 9.6 mmol) was added slowly at 0 °C to a solution of (*tert*-butyldimethylsilyl)(2-pyridylmethyl)amine (**1**) (2.12 g, 9.53 mmol) in 10 mL of toluene. After 15 h stirring at room temperature the volume of the dark solution was reduced to a few milliliters. Storage at 5 °C led to the precipitation of colorless crystals of **2**; yield: 2.13 g (3.53 mmol of dimeric **2**), 74%. − M.p. 136 °C. − NMR spectroscopic data are listed in Table 2. − IR: $\tilde{\nu} = 1641$ cm$^{-1}$ vw, 1606 vs, 1593 s, 1572 vs, 1553 sh, 1485 vs, 1474 s, 1431 vs, 1408 vs, 1387 s, 1355 s, 1320 w, 1283 s, 1253 vs, 1208 m, 1154 s, 1148 s, 1125 s, 1105 m, 1084 m, 1059 s, 1045 vs, 1022 s, 1007 s, 994 s, 960 s, 936 m, 886 sh, 829 vs, 814 sh, 771 vs, 719 s, 675 sh, 661 vs, 637 s, 617 s, 564 m, 499 s, 460 s, 446 s, 415 s, 403 m, 389 s, 364 m, 327 w, 286 vw. − $[C_{13}H_{24}N_2SiZn]_2$ (603.624): calcd. C 51.73, H 8.02, N 9.28; found C 51.09, H 7.90, N 9.34.

**Zinc Complex 3. − Method A (Thermal Decomposition of 2):** Compound **2** was heated without a solvent for 2 h at 150 °C. The evolving gas was collected and identified as methane by mass spectrometry. During the thermal decomposition reaction zinc metal precipitated. The NMR spectroscopic investigation confirmed the formation of **1**, **3**, and **4**, and small amounts of unchanged **2** were still

present. Compounds **1** to **4** were dissolved in hydrocarbons and separated from the insoluble materials. X-ray powder diffraction analysis of the residue verified the elimination of zinc metal, which was formed in an equimolar amount to the C−C coupling product **3**.

**Method B (C−C Coupling Reaction):** To a solution of 3.57 g of (*tert*-butyldimethylsilyl)(2-pyridylmethyl)amine (**1**) (16.1 mmol) in 20 mL of toluene was added 12.0 mL of a 2.0 M solution of dimethylzinc in toluene. The quantitative formation of **2** was confirmed by $^1$H NMR measurements. The reaction mixture was heated under reflux for 5 h. During this time zinc metal precipitated. The solution was filtered and the volume of was reduced to a few milliliters. On cooling the solution to −18 °C colorless crystals of **3** precipitated in the shape of small grains of rice; yield: 6.49 g (10.79 mmol), 67%. − Physical data: M.p. 191 °C. − NMR spectroscopic data are listed in Table 2. − IR: $\tilde{\nu}$ = 1642 cm$^{-1}$ vw, 1631 vw, 1602 vs, 1495 vw, 1474 vs, 1463 s, 1441 vs, 1408 m, 1386 m, 1357 m, 1348 m, 1331 w, 1290 m, 1279 m, 1249 vs, 1229 sh, 1212 w, 1186 vw, 1154 vs, 1106 m, 1060 vs, 1045 vs, 1020 vs, 1007 s, 936 vs, 890 m, 870 m, 844 s, 827 vs, 807 vs, 771 vs, 753 vs, 730 sh, 675 vs, 664 vs, 641 vs, 606 s, 573 vw, 557 sh, 544 m, 528 vs, 462 s, 437 s, 410 m, 378 w, 314 vw, 292 w, 274 w. − $C_{26}H_{46}N_4Si_2Zn_2$ (601.608): calcd. C 51.90, H 7.71, N 9.32; found C 52.01, H 7.81, N 9.32.

**Zinc Complex 4:** A 1.6 M solution of *n*-butyllithium (4.89 mL) in diethyl ether was added slowly at −78 °C to a solution of (*tert*-butyldimethylsilyl)(2-pyridylmethyl)amine (**1**) (1.74 g, 7.82 mmol) in 10 mL of tetrahydrofuran. A solution of zinc dibromide (0.88 g, 3.91 mmol) in 5 mL of tetrahydrofuran was added to the reaction solution at 0 °C. The mixture was stirred for 10 h, the solvent was removed and the residue was extracted with pentane. Recrystallization yielded colorless **4**; yield: 0.70 g (1.37 mmol), 35%. − M.p. 114 °C. − NMR spectroscopic data are listed in Table 2. − IR: $\tilde{\nu}$ = 3414 cm$^{-1}$ w, 3377 w, 1636 vw, 1604 s, 1594 sh, 1570 m, 1481 s, 1471s 1433 s, 1406 m, 1386 w, 1348 m, 1280 s, 1246 s, 1220 sh, 1211 w, 1151 m, 1122 vs, 1102 s, 1045 s, 1018 m, 1005 m, 994 sh, 982 sh, 927 s, 830 vs, 813 sh, 777 sh, 764 vs, 754 sh, 721 m, 671 sh, 657 m, 645 w, 614 w, 566 vw, 513 w, 486 vw, 469 vw, 454 vw, 429 sh, 407 w, 375 w, 351 w, 297 vw. − $C_{24}H_{42}N_4Si_2Zn$ (508.176): calcd. C 56.72, H 8.33, N 11.03; found C 56.72, H 8.33, N 11.03.

**X-ray Structure Determinations of 2 and 3:** Data were collected on a Siemens P4 diffractometer with a Siemens SMART−CCD area detector with graphite monochromated Mo-$K_\alpha$ radiation ($\lambda$ = 71.073 pm) using oil-coated, rapidly cooled single crystals.[15] Crystallographic parameters and details of data collection and refinement procedures are summarized in Table 3.

The structures were solved by direct methods and refined with the software packages SHELXL-93 and SHELXL-97.[17] Neutral scattering factors were taken from Cromer and Mann[18] and for the hydrogen atoms from Stewart et al.[19] The non-hydrogen atoms were refined anisotropically. The H-atoms were considered with a riding model under restriction of ideal symmetry at the corresponding carbon atoms. Crystallographic data (excluding structure factors) for the structures of **2** and **3** has been deposited with the Cambridge Crystallographic Data Centre as supplementary publication no. CCDC-147824 for **2** and -147825 for **3**. Copies of the data can be obtained on application to CCDC, 12 Union Road, Cambridge CB2 1EZ, UK [E-mail: deposit@ccdc.cam.ac.uk].

Table 3. Crystallographic data of **2** and **3** as well as details of the structure solution and refinement procedures

| Compound | 2 | 3 |
|---|---|---|
| Empirical formula | $C_{13}H_{24}N_2SiZn$ | $C_{13}H_{23}N_2SiZn$ |
| Formula mass [gmol$^{-1}$] | 301.80 | 300.79 |
| $T$ [K] | 193(2) | 193(2) |
| Crystal system | triclinic | tetragonal |
| Space group[16] | $P\bar{1}$ (No. 2) | $I4_1cd$ (No. 110) |
| $a$ [pm] | 858.3(2) | 1873.6(1) |
| $b$ [pm] | 986.1(2) | 1873.6(1) |
| $c$ [pm] | 1060.7(2) | 1781.6(1) |
| α [°] | 72.413(3) | 90 |
| β [°] | 83.311(4) | 90 |
| γ [°] | 68.207(3) | 90 |
| $V$ [nm$^3$] | 0.7946(2) | 6.2542(6) |
| $Z$ | 2 | 16 |
| $d_{calcd.}$ [gcm$^3$] | 1.261 | 1.278 |
| $\mu$ [mm$^{-1}$] | 1.604 | 1.630 |
| $F$(000) | 320 | 2544 |
| Scan range [°] | $4.0 < 2\theta < 58.5$ | $4.3 < 2\theta < 58.6$ |
| Measured data | 4588 | 17200 |
| Unique data ($R_{int}$) | 2431 (0.0223) | 3277 (0.0356) |
| Absorption. corr. | semiempirical | semiempirical |
| Max./min. transmission | 0.7397/0.5662 | 0.7363/0.6405 |
| Parameters | 160 | 160 |
| Restraints | 0 | 1 |
| $wR_2$[a] (all data, on $F^2$) | 0.2061 | 0.0593 |
| $R_1$[a] (all data) | 0.0706 | 0.0307 |
| Flack parameter | − | 0.007(9) |
| Data with $I > 2\sigma(I)$ | 2157 | 2952 |
| $R_1$ [$I > 2\sigma(I)$] | 0.0652 | 0.0247 |
| Gof $s$[b] on $F^2$ | 1.126 | 1.025 |
| Residual dens. [enm$^{-3}$] | 1303/−708 | 301/−277 |
| CCDC number | CCDC-147824 | CCDC-147825 |

[b] $s = \{\Sigma[w(F_o^2 - F_c^2)^2]/(N_o - N_p)\}^{1/2}$.

## Acknowledgments

This work was financially supported by the Deutsche Forschungsgemeinschaft, Bonn, and the Fonds der Chemischen Industrie, Frankfurt/Main. We thank Mr. S. Correll for performing the X-ray powder diffraction experiments. T. Bollwein wishes to express his gratitude to the Fonds der Chemischen Industrie for a Ph. D. scholarship.

[1] For examples see: K.-H. Thiele, J. Köhler, *Z. Anorg. Allg. Chem.* **1965**, *337*, 260−267; K.-H. Thiele, H. Rau, *Z. Anorg. Allg. Chem.* **1967**, *353*, 127−134; H. Rau, K.-H. Thiele, *Z. Anorg. Allg. Chem.* **1967**, *355*, 253−264; K. J. Fisher, *Inorg. Nucl. Chem. Lett.* **1973**, *9*, 921−925; J. Behm, S. D. Lotz, W. A. Herrmann, *Z. Anorg. Allg. Chem.* **1993**, *619*, 849−852; J. Pickard, B. Straub, *Z. Naturforsch.* **1995**, *50b*, 1517; H. Gornitzka, C. Hemmert, G. Bertrand, M. Pfeiffer, D. Stalke, *Organometallics* **2000**, *19*, 112−114.

[2] J. G. Noltes, J. Boersma, *J. Organomet. Chem.* **1967**, *9*, 1−4; A. J. de Koning, J. Boersma, G. J. M. van der Kerk, *J. Organomet. Chem.* **1980**, *186*, 159−172; E. Wissing, M. Kaupp, J. Boersma, A. L. Spek, G. van Koten, *Organometallics* **1994**, *13*, 2349−2356.

[3] M. Westerhausen, B. Rademacher, W. Schwarz, *J. Organomet. Chem.* **1992**, *427*, 275−287; M. Westerhausen, B. Rademacher, *J. Organomet. Chem.* **1993**, *443*, 25−33.

[4] P. C. Andews, C. L. Raston, B. W. Skelton, A. H. White, *Organometallics* **1998**, *17*, 779−782.

[5] W. Kaim, *Chem. Ber.* **1981**, *114*, 3789; M. Westerhausen, B. Rademacher, in *The Chemistry of the Copper and Zinc Triads* (Eds.: A. J. Welch, S. K. Chapman), The Royal Society of Chemistry, Cambridge, **1993**, pp. 148−151.

[6] E. Kimura, *Prog. Inorg. Chem.* **1994**, *41*, 443. For recent examples see: A. Looney, G. Parkin, R. Alsfasser, M. Ruf, H. Vahrenkamp, *Angew. Chem.* **1992**, *104*, 57−58; *Angew. Chem. Int. Ed. Engl.* **1992**, *31*, 92−93; M. Ruf, F. A. Schell, R. Walz, H.

Vahrenkamp, *Chem. Ber./Recueil* **1997**, *130*, 101−104; M. Rombach, C. Maurer, K. Weis, E. Keller, H. Vahrenkamp, *Chem. Eur J.* **1999**, *5*, 1013−1027.
[7] G. van Koten, J. T. B. H. Jastrzebski, K. Vrieze, *J. Organomet. Chem.* **1983**, *250*, 49−61.
[8] J. T. B. H. Jastrzebski, J. M. Klerks, G. van Koten, K. Vrieze, *J. Organomet. Chem.* **1981**, *210*, C49−C53.
[9] M. Kaupp, H. Stoll, H. Preuss, W. Kaim, T. Stahl, G. van Koten, E. Wissing, W. J. J. Smeets, A. L. Spek, *J. Am. Chem. Soc.* **1991**, *113*, 5606−5618; E. Wissing, M. Kaupp, J. Boersma, A. L. Spek, G. van Koten, *Organometallics* **1994**, *13*, 2349−2356; E. Wissing, E. Rijnberg, P. A. van der Schaaf, K. van Gorp, J. Boersma, G. van Koten, *Organometallics* **1994**, *13*, 2609−2615; E. Wissing, K. van Gorp, J. Boersma, G. van Koten, *Inorg. Chim. Acta* **1994**, *220*, 55−61.
[10] A. L. Spek, J. T. B. H. Jastrzebski, G. van Koten, *Acta Cryst.* **1987**, *C43*, 2006−2007; E. Wissing, S. van der Linden, E. Rijnberg, J. Boersma, W. J. J. Smeets, A. L. Spek, G. van Koten, *Organometallics* **1994**, *13*, 2602−2608.
[11] E. Rijnberg, B. Richter, K.-H. Thiele, J. Boersma, N. Veldman, A. L. Spek, G. van Koten, *Inorg. Chem.* **1998**, *37*, 56−63.
[12] M. S. Chinn, J. Chen, *Inorg. Chem.* **1995**, *34*, 6080−6084.
[13] M. Westerhausen, T. Bollwein, K. Polborn, *Z. Naturforsch.* **2000**, *55b*, 51−59.
[14] A. Haaland, K. Hedberg, P. P. Power, *Inorg. Chem.* **1984**, *23*, 1972−1975; P. P. Power, K. Ruhlandt-Senge, S. C. Shoner, *Inorg. Chem.* **1991**, *30*, 5013−5015; W. S. Rees, D. M. Green, W. Hesse, *Polyhedron* **1992**, *11*, 1697−1699; M. A. Putzer, A. Dashti-Mommertz, B. Neumüller, K. Dehnicke, *Z. Anorg. Allg. Chem.* **1998**, *624*, 263−266; W. S. Rees, O. Just, H. Schumann, R. Weimann, *Polyhedron* **1998**, *17*, 1001−1004; H. Schumann, J. Gottfriedsen, S. Dechert, F. Girgsdies, *Z. Anorg. Allg. Chem.* **2000**, *626*, 747−758.
[15] T. Kottke, D. Stalke, *J. Appl. Crystallogr.* **1993**, *26*, 615−619; D. Stalke, *Chem. Soc. Rev.* **1998**, *27*, 171−178.
[16] *International Tables for Crystallography* (Ed.: T. Hahn), Vol. A, *Space Group Symmetry*, 2nd Ed., D. Reidel, Dordrecht, **1984**.
[17] G. M. Sheldrick, *SHELXL-93*, Universität Göttingen, **1993**; *SHELXL-97*, Universität Göttingen, **1997**.
[18] D. T. Cromer, J. B. Mann, *Acta Crystallogr.* **1968**, *24*, 321−324.
[19] R. F. Stewart, E. R. Davidson, W. T. Simpson, *J. Chem. Phys.* **1965**, *42*, 3175−3187.

Received August 4, 2000
[I00308]